ALGEBRAIC COLLECTIVE MODEL AND NUCLEAR STRUCTURE APPLICATIONS

G. Thiamova, M. Abolghasem

LPSC, Université Grenoble-Alpes, CNRS/IN2P3
53, rue des Martyrs, 38026 Grenoble Cedex, France

(Received December 18, 2013; revised version received March 19, 2014; final version received June 18, 2014)

We present results that can be obtained with an algebraic version of Bohr's collective model with the aim to identify the limitations of the model as much as it successes. A special focus is placed on the analysis of triaxial nuclei. The first, simple application of the algebraic collective model to ^{188,192}Os is performed with the aim to identify, among the observed $J = 0^+$ states, the best candidates for a β vibration. A conclusion of this analysis is that beta bandheads in these nuclei are to be expected at a much higher energy than the energy of the observed 0_2 states. This finding is in agreement with the vibration-rotation model predictions and the predictions of the symplectic model. A decisive role played by β and γ fluctuations for a correct description of the amplitudes of the quasi-γ-band staggerings is shown. In particular, it is revealed that β fluctuations act differently in the axially symmetric and the triaxial regime.

DOI:10.5506/APhysPolB.45.1833
PACS numbers: 21.60.Ev, 21.60.Fw

1. Introduction

The Bohr collective model (BM) [1] and its many extensions [2] serve as a basic tool for understanding and description of collective degrees of freedom in nuclei. Alternatively, the interacting boson model (IBM) [3] can be used which capitalizes on its algebraic structure to provide an effective and quick characterization of experimental data. The algebraic collective model (ACM) [4], introduced as a computationally tractable version of the BM restricted to rotational and quadrupole vibrational degrees of freedom, is also characterized by a well defined algebraic structure (see Ref. [5] for a review of this model) and as such it combines the advantages of both the BM and the IBM. In fact, its algebraic structure makes collective model in the ACM calculations a simple routine procedure. Many examples showing

the diversity of the results obtainable with the ACM have been displayed in detail in [4]. Their work did not aim at analyzing a particular set of experimental data but rather at providing a general view of the results that can be obtained.

On the other hand, a primary focus of this paper is to look at the capability of the ACM to provide a realistic description of deformed nuclei, both in the axially symmetric and in the triaxial regime. As the experimental quasi-γ-band staggerings in different isotopic chains have turned out to be a very sensitive signature of the presence of diverse nuclear shapes, it is of interest to investigate how their theoretical counterparts depend on the model parameters. It is shown that they are especially sensitive to the degree of β fluctuations and, more interestingly, that β fluctuations act in an opposite way in the axially symmetric and in the triaxial regime.

As the first application of the ACM we have chosen to analyze ^{188,192}Os. The Os isotopes have been a subject of many theoretical and experimental studies that focused on a description of the structure of those complex transitional nuclei. In particular, the presence of triaxial shapes and the prolate-to-oblate transition in the Os isotopic chain made it an interesting and challenging topic of study. The microscopic and semimicroscopic models [6–12] usually predict γ-soft or γ-unstable ground state intrinsic shapes in the Os–Pt region. It implies that very shallow minima in the γ direction are to be expected. Moreover, Kumar [13] predicted that Os isotopes are prolate up to $A = 192$ and then suddenly change to oblate for heavier masses. Casten and Cizewski [14] deduced from the excitation spectra and γ-decay systematics that the prolate-to-oblate transition happens almost suddenly at $A = 194$ in the Os isotopes. Ground state potential energy surfaces (PES) for the Os and Pt isotopes have been obtained using the self-consistent Hartree–Fock–Bogoliubov (HFB) calculations based on a microscopic effective nucleon–nucleon interaction in Refs. [15, 16]. Study of such energy surfaces as a function of the deformation parameters β and γ has revealed that the Os isotopes possess a prolate shape with a flat potential in γ for $^{186-192}$Os. The HFB analysis applied to several isotopes of Yb, Hf, W, Os and Pt has confirmed that when the neutron number is increased the ground-state shapes evolve from axially symmetric prolate shapes to axially symmetric oblate shapes. It has also revealed the existence of a very shallow triaxial minimum for the transitional $N \sim 116$ nuclei [17]. A triaxiality in ^{188,190,192}Os has been investigated within the liquid drop Hamiltonian amended with a potential separable in β and γ coordinates in Ref. [18]. A solution of the BM Hamiltonian for soft triaxial nuclei has been obtained in Ref. [19] which employs a potential separable in β and γ and an application to Os isotopes has been considered. A rigid triaxial rotor model was applied to the description of E2 properties of ^{186,188,190,192}Os in Ref. [20].

The aim of the ACM analysis of ^{188,192}Os is not so much to compete with the existing theoretical calculations of Os isotopes but rather to examine the data from a perspective of a simple model and to determine when it breaks down. We will perform several fits of the spectrum of each nucleus in which beta bandheads will be identified with one of the observed $J = 0^+$ states. The aim of such an analysis is to find which of those states would fit the best properties expected for a β vibration. A significant conclusion that arises from the analysis is that the real β bands in these nuclei, if they exist, probably lie at a much higher energy than the energy of the observed 0_2 states. As we discuss below, this result is consistent with a symplectic model prediction [21, 22] and with the experimental characterization of the β vibration in deformed nuclei [23].

The ACM is briefly introduced in the next section. In the third section the calculations are presented and in the discussion section we raise some important questions that would deserve a further investigation.

2. ACM model calculations

The ACM, introduced as a computationally tractable version of the BM [1] restricted to rotational and quadrupole vibrational degrees of freedom, is characterized by a well defined algebraic structure. Unlike the conventional U(5) $\supset$ SO(5) $\supset$ SO(3) dynamical subgroup chain used, for example, in the Frankfurt program [24, 25], the ACM makes use of the subgroup chain

$$\mathrm{SU}(1,1) \times \mathrm{SO}(5) \supset \mathrm{U}(1) \times \mathrm{SO}(3) \supset \mathrm{SO}(2) \tag{1}$$

to define basis wave functions as products of β wave functions and SO(5) spherical harmonics. Several advantages result from this choice of dynamical subgroup chain: *(i)* with the now available SO(5) Clebsch–Gordan coefficients [26, 27], and explicit expressions for SO(5) reduced matrix elements, matrix elements of BM operators can be calculated analytically; *(ii)* by appropriate choices of SU(1,1) modified oscillator representations, the β basis wave functions range from those of the U(5) $\supset$ SO(5) harmonic vibrational model to those of the rigid-beta wave function of the SO(5)-invariant Wilets–Jean model; and *(iii)* with these SU(1,1) representations, collective model calculations converge an order of magnitude more rapidly for deformed nuclei than in U(5) $\supset$ SO(5) bases. Thus, the ACM combines the advantages of the BM and the IBM and makes collective model calculations a simple routine procedure [4, 28–30].

In the ACM, fully converged calculations were performed in Ref. [4] for a range of Hamiltonians to determine the extent to which experimental data can be realistically described in terms of the BM. More importantly,

they prepare the way for more general, but still solvable, algebraic collective models that include intrinsic degrees of freedom as in the unified model of Bohr and Mottelson [2, 31–34].

A detailed description of the ACM model can be found in Ref. [4]. A general purpose ACM Hamiltonian is given, for example, in the form

$$\hat{H}(M,\alpha,\kappa,\chi) = \frac{-\nabla^2}{2M} + \frac{1}{2}M\left[(1-2\alpha)\beta^2 + \alpha\beta^4\right] - \chi\beta\cos 3\gamma + \kappa\cos^2 3\gamma\,, \quad (2)$$

where

$$\nabla^2 = \frac{1}{\beta^4}\frac{\partial}{\partial\beta}\beta^4\frac{\partial}{\partial\beta} + \frac{1}{\beta^2}\hat{\Lambda} \quad (3)$$

is the Laplacian on the 5-dimensional collective model space [5]. Such a Hamiltonian, expressed in terms of the quadrupole deformation parameters β and γ serves as a useful starting point for a description of a wide range of nuclear collective spectra. A Hamiltonian of this form was used, for example, to study the second-order phase transition of a model nucleus, from a spherical to a deformed phase, with α as a control parameter [32]. For $\alpha = 0$, the potential is that of a spherical harmonic oscillator, $\frac{1}{2}M\beta^2$, while for $\alpha > 0.5$ it has a minimum for a non-zero value of β, which increases as α increases. Moreover, as the mass parameter M of the Hamiltonian (2) increases, the kinetic energy decreases and the result is a decrease of the vibrational β fluctuations of the model about its equilibrium deformation. Thus, the value of the parameter α controls the β deformation of the model and the parameter M controls its rigidity. By adjusting the parameters α and M, a model with any equilibrium value of the β deformation and any degree of rigidity may be constructed. In Ref. [4] it has been shown that parameter values in the range $0 < \alpha < 2.0$ and $10 < M < 100$ are sufficient to describe the β deformations and rigidities of the observed nuclear collective states.

The terms β^2 and $\cos 3\gamma$ in Eq. (2) are defined in terms of the quadrupole tensor operator $\hat{Q}$ by

$$\hat{Q}\cdot\hat{Q} = \beta^2\,, \qquad \left(\hat{Q}\otimes\hat{Q}\otimes\hat{Q}\right)_0 = -\sqrt{\frac{2}{35}}\,\beta^3\cos 3\gamma\,. \quad (4)$$

The last term in Hamiltonian (2), proportional to $\cos^2 3\gamma$, can induce a triaxial minimum in the PES. A delicate competition between all the three terms in the potential and the second and the third one, in particular, will determine whether the potential energy minimum will remain axially spherical (second term proportional to $\cos 3\gamma$ dominates) or will be driven to a triaxial minimum by the last term.

It should be noted that the prolate-to-oblate transition is obtained trivially by changing the sign of the parameter χ and this sign change does not produce any effect on the calculated spectra as the Hamiltonian (2) is isospectral with regard to this sign transformation.

Several fits for each of the two nuclei are performed in which β bandheads are identified with one of the observed $J = 0^+$ levels. Thus, in each fit the energy of the calculated $J = 0_2$ state should match as much as possible the energy of a particular $J = 0_n$ state and, at the same time, the energies of the ground band and the γ band are optimized. Moreover, we pay an attention to a good reproduction of the γ-band staggerings which are known to be characteristic of the standard structural limits. To minimize a deviation of the experimental and calculated energy values, a least-square method has been used in a suitable part of the multidimensional parameter space defined above. The procedure was carried out in two steps. First, coarse-grain fits were performed to narrow down the parameter space to a physically meaningful subspace. In the second step, fine-grain fits were done with steps $\Delta M = 0.5$, $\Delta\alpha = 0.1$, $\Delta\chi = 0.1$ and $\Delta\kappa = 0.1$ to obtain final results.

3. Results

In this section, the results obtained with the ACM Hamiltonian (2) are presented. First, in Figs. 1 (a)–(f) and 2 (a)–(c) fits of the energy levels of ^{188}Os and ^{192}Os taken from Ref. [35] are shown in which the observed $J = 0_n$ states are supposed to represent candidates for a β vibration.

A striking feature of the calculation is a large amount of the centrifugal stretching present when the lowest $J = 0_n$ states are included in the fit. It is manifested by the fact that the calculated energies of the ground band levels fall increasingly below the experimental ones as the angular momentum increases. In fact, a large centrifugal stretching is to be expected for small values of the mass parameter M for which the β and γ bands appear in the low-energy spectrum [4]. In the adiabatic approximation of the BM, the centrifugal stretching is neglected on the assumption that the β and γ excitations appear high in energy and thus decouple from the rotational motion. The increasing E2 transition rates over the experimental values is another evidence of the centrifugal stretching. This is traditionally understood as a result of an increasing deformation β which implies an increase of the rotational moment of inertia with increasing angular momentum. Interestingly, deviations from the $J(J+1)$ spectrum have been noted also within a β-rigid calculation in Ref. [33], where the effect arises purely from the interaction of the γ and the rotational degrees of freedom. Thus in the context of a calculation considered in this paper, in which the potential is not β rigid anymore, those deviations must be interpreted as a result of a softness of the potential

both in the β and γ direction. We observe that the centrigugal stretching gradually diminishes with increasing energy of $J = 0_n$ states indicating that β vibrations, if they exist, should be expected at higher excitation energies.

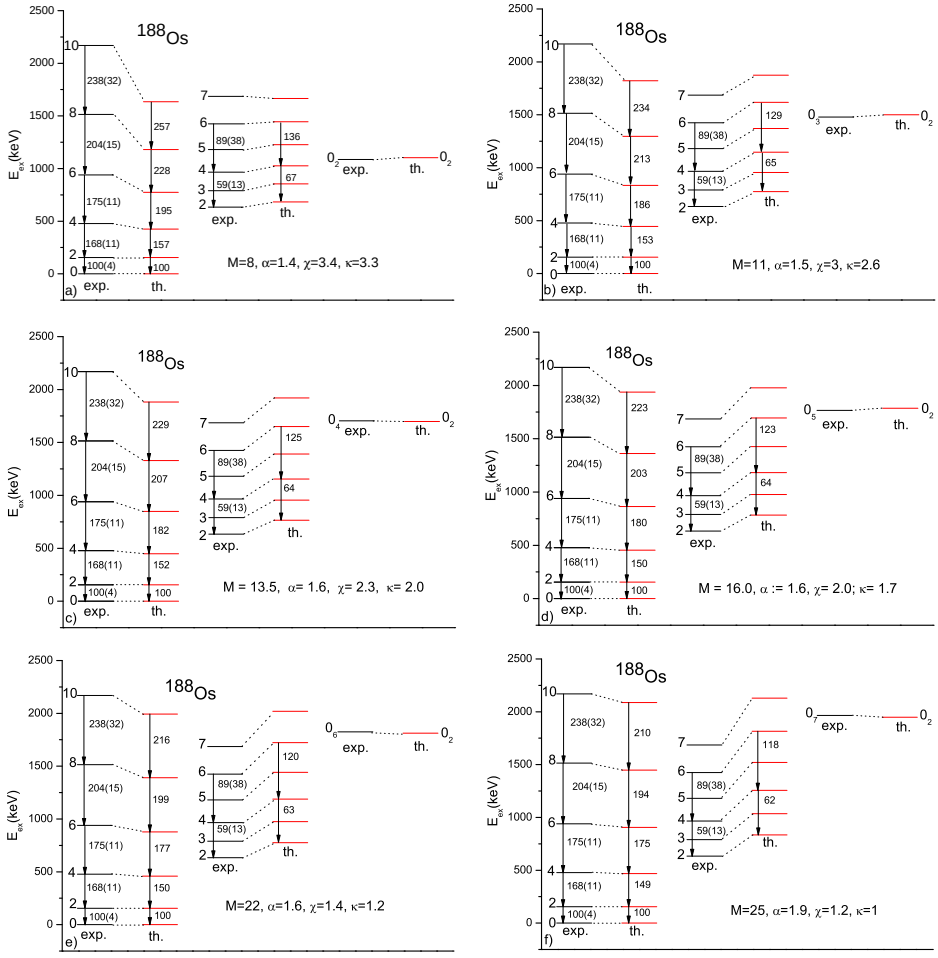

Fig. 1. Experimental and calculated spectra of ^{188}Os. In each figure, the $J = 0_n$ state included in the fit is indicated. E2 transition rates are shown as percentages of those for the $2_1 \to 0_1 = 100$ transitions. Experimental errors are indicated in the parenthesis. In the case of asymmetric errors, they are shown as an upper and a lower index of the corresponding transition.

The interband E2 transition rates are shown in Figs. 3 (a)–(f) for ^{188}Os and in Figs. 4 (a)–(c) for ^{192}Os. Some of the $\gamma \to$ ground band transitions in ^{188}Os are less correctly described. We also observe that the E2 transition rate from the 0_2 state to the 2_1 state is too strong in comparison with the

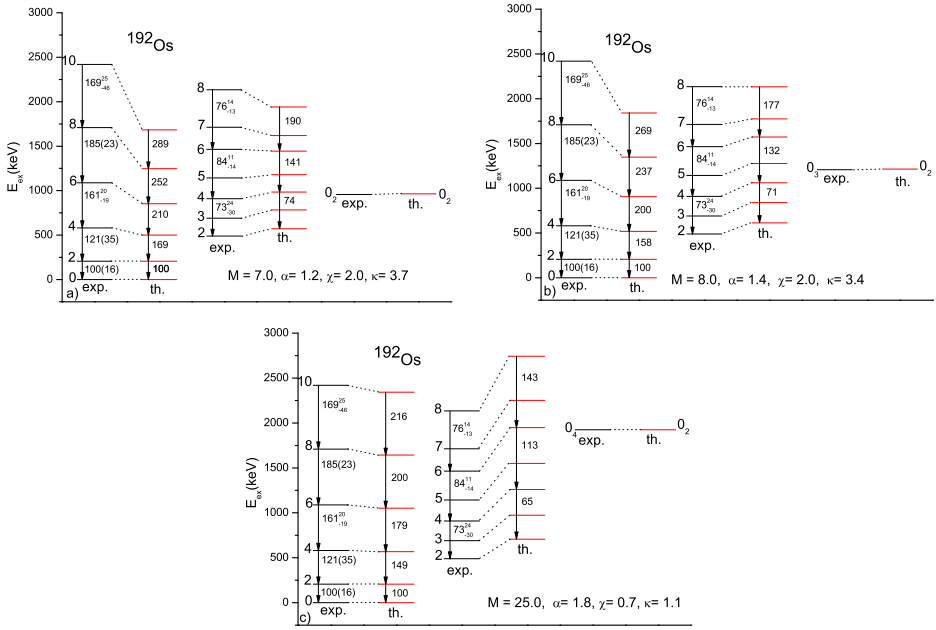

Fig. 2. Experimental and calculated spectra of ^{192}Os. In each figure, the $J = 0_n$ state included in the fit is indicated. E2 transition rates are shown as percentages of those for the $2_1 \to 0_1 = 100$ transitions. Experimental errors are indicated in the parenthesis. In the case of asymmetric errors, they are shown as an upper and a lower index of the corresponding transition.

experimental value. In the case of ^{192}Os, all the interband transition rates are well reproduced except the E2 transition rate from the 0_2 state to the 2_1 which is again too strong. However, we observe, that this particular transition in both nuclei decreases with increasing energy of the $J = 0_n$ states included in the fits. It is instructive to see whether such a behavior is consistent with predictions of the macroscopic liquid drop model from which β and γ vibrations originate. Using experimentally determined deformation parameters β_0 and moments of inertia J_0 various quantities can be calculated. One of them is the ratio R of the E2 transition rates for $0_\beta \to 2_1$ and $2_\gamma \to 0_1$ transitions for which we obtain [23]

$$R = 5y^2 \frac{(1+2\alpha)^2}{x^2(1-2\alpha)^2}\,, \tag{5}$$

where $\alpha = \frac{2}{7}\sqrt{\frac{5}{\pi}}\,\beta_0$, $x = \sqrt{\frac{3\hbar^2}{J_0 E_\gamma}}$ and $y = \sqrt{\frac{3\hbar^2}{2J_0 E_\beta}}$.

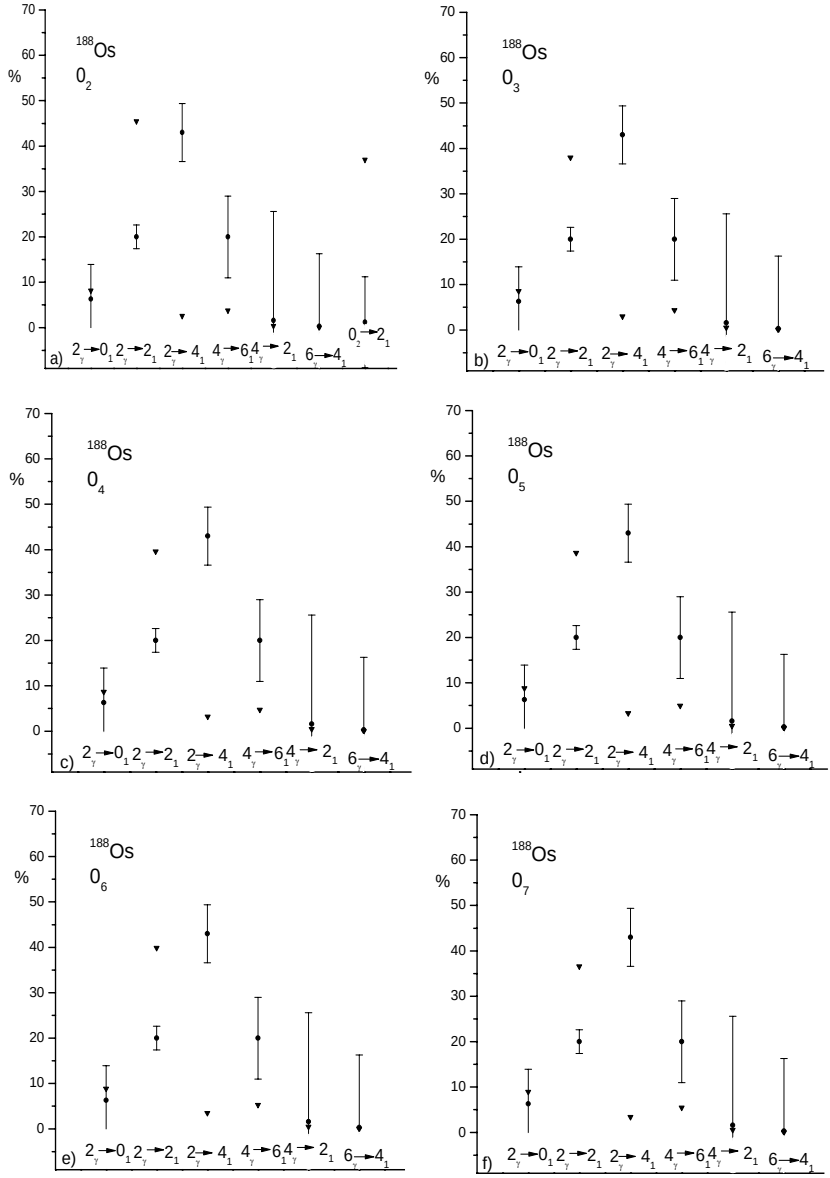

Fig. 3. Known experimental interband transition rates (circles) and their calculated counterparts (triangles) for ^{188}Os are shown as percentages of the $2_1 \to 0_1 = 100$ transitions.

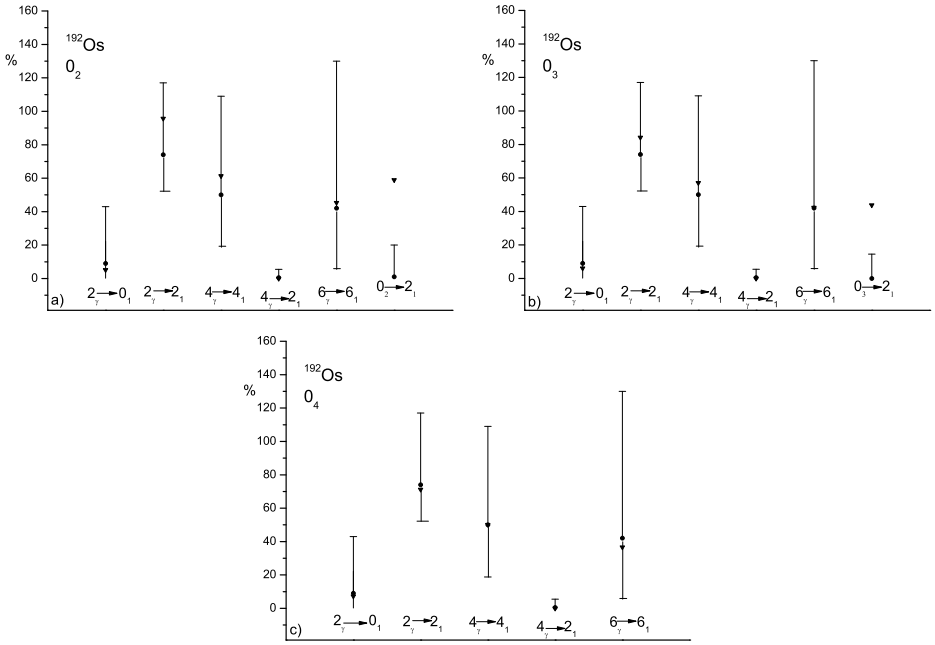

Fig. 4. Known experimental interband transition rates (circles) and their calculated counterparts (triangles) for ^{192}Os are shown as percentages of the $2_1 \to 0_1 = 100$ transitions.

In the absence of serious mixing, this ratio gives a guideline as to what to expect for a β vibration. Taking $\beta_0 = 0.192$ [36] and $\frac{\hbar^2}{2J_0} = 25.83$ keV for ^{188}Os and $\beta_0 = 0.155$ [36] and $\frac{\hbar^2}{2J_0} = 34.33$ keV for ^{192}Os, we obtain the macroscopic liquid drop model predictions (MLD) as shown in Figs. 5 (a) and (b). Each MLD value in Fig. 5 has been obtained by replacing E_β by the energy of the $J = 0_n$ state included in the fit and by replacing E_γ by the energy of the observed γ bandhead. By comparing the MLD predictions with their ACM counterparts, it is clearly seen that the ACM values decrease with increasing energy of $J = 0_n$ states and approach the respective MLD estimates. In the case of ^{188}Os, the best agreement between the MLD and ACM values is reached for the $J = 0_4$ excited state at 1704 keV, for which however, the centrifugal stretching present in the spectrum is still quite large. In the case of ^{192}Os, the best agreement is obtained for 0_4 excited state at 1924 keV for which the centrifugal stretching is very small. Thus this state may be a good candidate for a β vibration in ^{192}Os.

Another guideline as to which state may be a good candidate for a β vibration is obtained by analyzing E0 transition rates. Wood *et al.* [37] have given a detailed account of both experimental and theoretical E0 properties. They have pointed out that the β vibration should give rise to enhanced

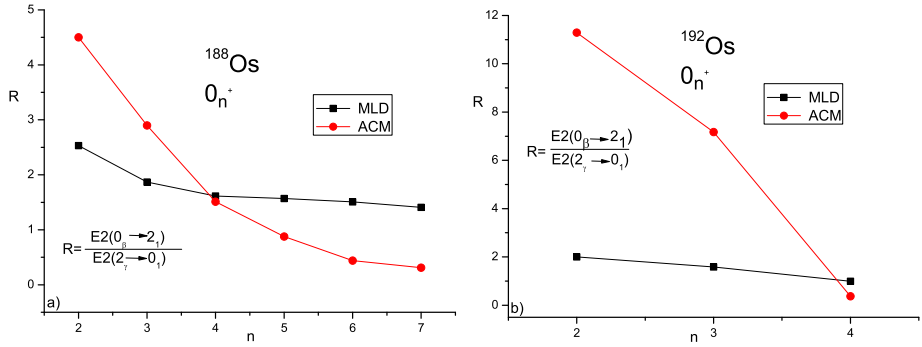

Fig. 5. Ratios R of the $0_\beta \to 2_1$ and the $2_\gamma \to 0_1$ transitions obtained within the ACM and the MLD model for (a) ^{188}Os and (b) ^{192}Os. The index n indicates which of the $J = 0_n$ state has been included in the fit. See the text for details.

E0 transitions to the ground state due to the radial shape oscillations in β. Such transitions from the levels $J = 0_n$, $n = 4, 5, 6$ and 7 have, indeed, been observed [38]. Thus, even though the ACM analysis is not conclusive enough in the case of ^{188}Os to pick out a single candidate for a β vibration, the results clearly show that a β vibration, if it exists, should be looked for at the energies exceeding 1700 keV.

Interestingly, the vibration-rotation model predicts the energy of the β bandhead in ^{188}Os at 1700 keV [39]. Also, in the symplectic model, the lowest collective states are the renormalized SU(3) states which have no 0_2 excitations. Low-energy 0_2 excitations should then come from other representations and have non-zero transitions to the ground state band due to band (representation) mixing [21, 22]. The calculations within the quasiparticle phonon model (QPM) [40] have also confirmed that the 0_2^+ states in ^{188,190,192}Os do not exhibit the typical properties of β-vibrational bands [41]. The 0^+ states turn out to be linear combinations of several QRPA 0^+ phonons. Moreover, the 0_2^+ state contains a large two-phonon $\gamma\gamma$ component which increases from ^{188}Os to ^{190,192}Os. This feature can also be linked to the proximity of the γ-soft region.

Another interesting feature that arises from the calculations is that the potential energy surfaces (PES) become increasingly γ-soft with increasing energy of the $J = 0_n$ states as is seen in Figs. 6 and 7. This is in agreement with other theoretical calculations discussed in the introduction that predict γ-soft or γ-unstable ground state intrinsic shapes in the Os–Pt region. Thus, the nuclei seem to resemble more closely the Wilets–Jean γ-independent limit [42].

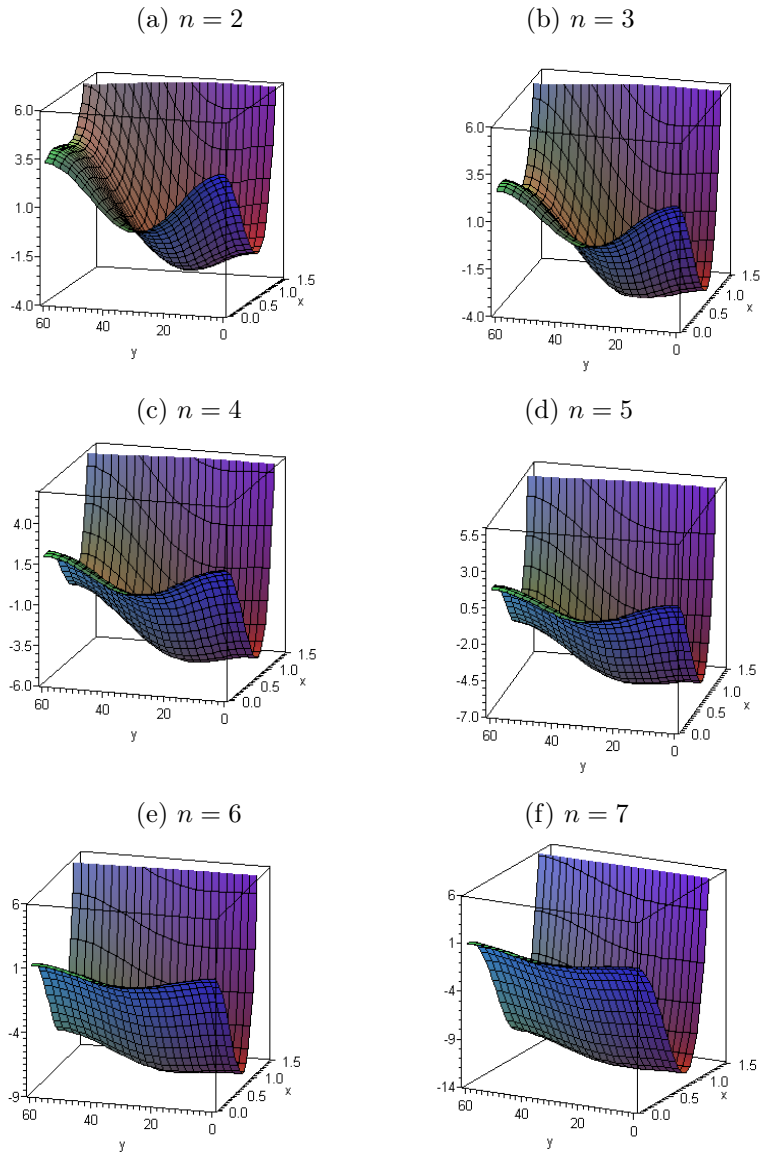

Fig. 6. Potential energy surfaces obtained for ^{188}Os and the Hamiltonian parameters as in Figs. 1 (a)–(f). The index n indicates which of the $J = 0_n$ state has been included in the fit. The values of the deformation parameter γ are shown on the y axis, while the x axis represents the deformation parameter β.

One undesirable feature of the calculations is a shift of the γ band as a whole towards higher energies with increasing energy of the theoretical 0_2 state. This is also reflected by the values of $\sigma^2 = \sum_i (E_{\rm exp} - E_{\rm th})^2/N$ that

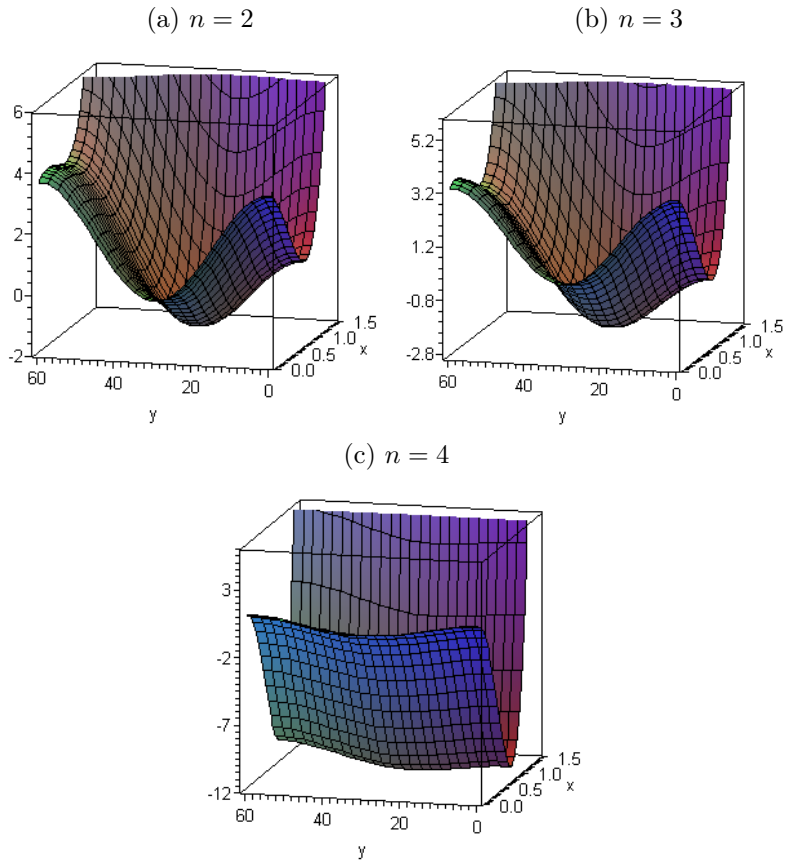

Fig. 7. Potential energy surfaces obtained for ^{192}Os and the Hamiltonian parameters as in Figs. 2 (a)–(c). The index n indicates which of the $J = 0_n$ state has been included in the fit. The values of the deformation parameter γ are shown on the y axis, while the x axis represents the deformation parameter β.

characterize the specific errors of the fits. N is the number of excited states. The values of σ are shown in Tables I and II for ^{188}Os and ^{192}Os, respectively. While in the axially symmetric regime the energy of the γ bandhead increases with increasing β and γ rigidity of the potential, in the triaxial regime it increases with increasing β rigidity and increasing γ softness of the potential. Since the PES of both nuclei posses a triaxial minimum that becomes more β rigid and more γ soft with increasing energy of the theoretical 0_2 state, the energy of the γ bandheads is shifted towards higher energies.

TABLE I

Values of σ (in MeV) characterizing the quantitative errors of the fitting procedure for ^{188}Os. The fits are marked by the $J = 0_n$ states included in the calculations.

^{188}Os						
0_i	0_2	0_3	0_4	0_5	0_6	0_7
σ_i	0.192	0.176	0.172	0.184	0.188	0.235

TABLE II

Values of σ (in MeV) characterizing the quantitative errors of the fitting procedure for ^{192}Os. The fits are marked by the $J = 0_n$ states included in the calculations.

^{192}Os			
0_i	0_2	0_3	0_4
σ_i	0.261	0.214	0.330

It is necessary to analyze more nuclei in this or other mass regions to see whether this feature of the calculation persists in other cases and is thus a weakness of the model employed or whether it is related to a more complex structure of the analyzed states that cannot be satisfactorily described by the present simple collective model.

It should be noted that a good description of the γ bands in the osmium isotopes has been a challenge also for the related IBM. In [43] not only have the γ bands systematically been shifted towards higher energies in some cases by 100 or 200 keV, but, unlike the present ACM calculations, the γ staggerings have not been correctly reproduced.

Another focus of this paper is an analysis of the experimental staggerings and the conditions under which their realistic description can be obtained. The experimental staggerings in different isotopic chains have revealed that different staggering patterns are characteristic of the standard structural analytical limits known in, for example, the IBM based models. One example can be nuclei that represent the transition between vibrational and γ-soft structures that show strong staggering with negative $S(J)$ values at even-J and positive $S(J)$ values at odd-J spins. The heavy rare-earth nuclei known to display an axially symmetric behavior show a similar staggering pattern with a smaller overall magnitude [44].

The staggering patterns of the quasi-γ bands are typically displayed using the quantity $S(J)$ defined as follows [45]

$$S(J) = \frac{(E(J) - E(J-1)) - (E(J-1) - E(J-2))}{E(2_1^+)}\,. \tag{6}$$

An irregular staggering pattern is observed for ^{188}Os which is well reproduced by all the calculations with parameters shown in Figs. 1 (a)–(f) (see Fig. 8). The staggering pattern of ^{192}Os is characteristic of a soft triaxial rotor with positive $S(J)$ values at even-J and negative $S(J)$ values at odd-J spins (see Fig. 9). It should be noted that large positive values $S(4)$ correspond to a rigid triaxial rotor, while the small experimental value for ^{192}Os reflects the softness of the potential in the γ direction. All sets of calculations reproduce the staggering pattern correctly and the ACM values of $S(J)$ are very close to their experimental counterparts. It should be noted that the staggering pattern of ^{192}Os has also been analyzed within a β-rigid

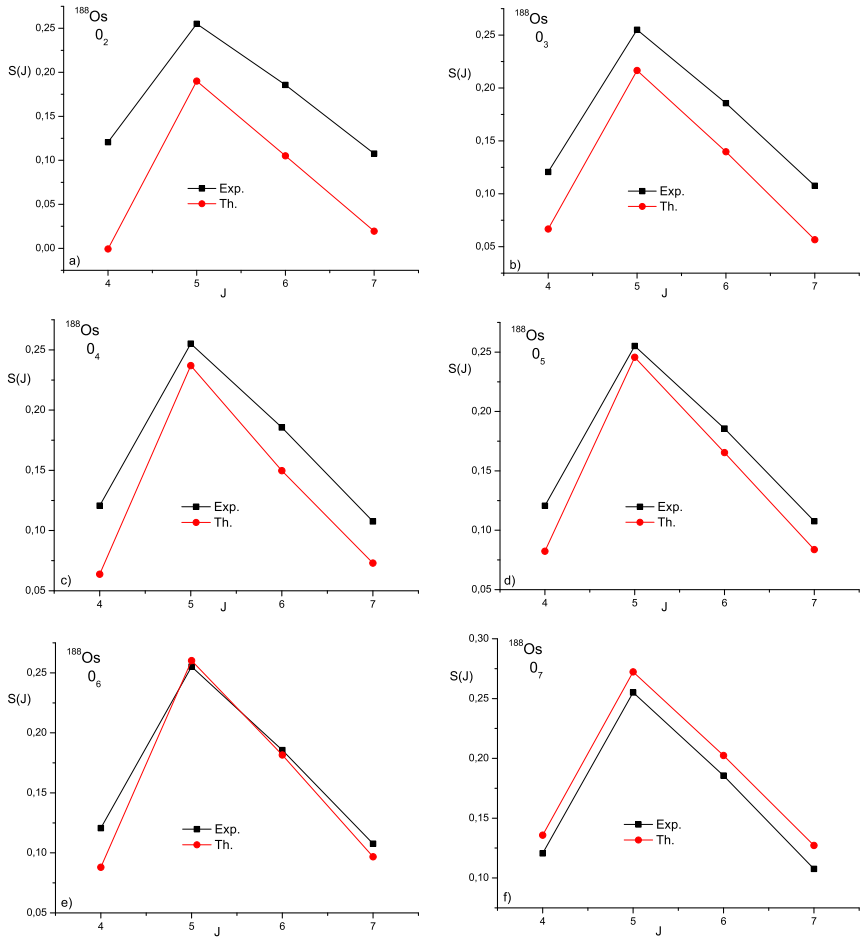

Fig. 8. Staggering patterns obtained for ^{188}Os and the Hamiltonian parameters as in Figs. 1 (a)–(f).

IBM calculation in Ref. [46] and the overall magnitude of the calculated staggering was much larger than the observed one. This comparison reveals the importance of β fluctuations for a realistic description of the data.

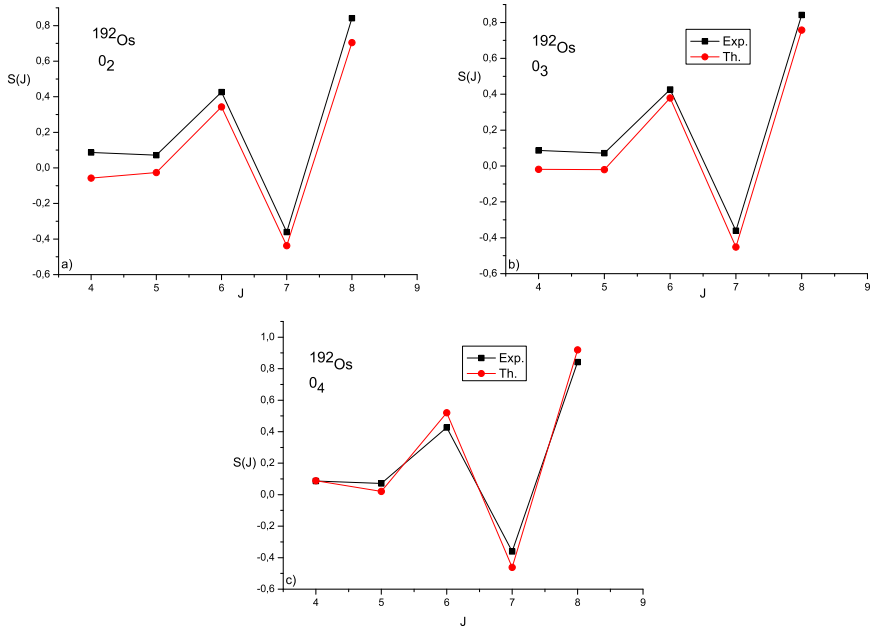

Fig. 9. Staggering patterns obtained for ^{192}Os and the Hamiltonian parameters as in Figs. 2 (a)–(c).

To demonstrate the role played by the β rigidity of the potential, we show in Fig. 10 several staggering patterns obtained for ^{192}Os. The Hamiltonian parameters are the same as in Fig. 2 (c), only the mass parameter M changes from one calculation to another. It can be clearly seen that larger parameters M that correspond to more β-rigid potentials lead to larger magnitudes of $S(J)$, while with decreasing value of M the magnitude of $S(J)$ decreases and the staggering pattern eventually becomes the one characteristic of an axially symmetric rotor.

To understand the mechanism by which this happens in the present model, it is convenient to use unphysically small values of M as shown in Fig. 11. A choice of such small values of M does not influence the qualitative conclusions but makes the changes of the PES better seen. We observe that as the parameter M decreases, the potential flattens more and more in the β direction as should be expected. At the same time, larger and larger values of β become accessible to the wave functions and, as a consequence, the importance of the term proportional to χ increases. This is the term

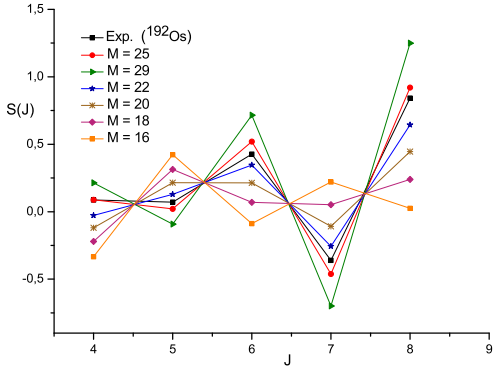

Fig. 10. Dependence of the quasi-γ-band staggering on the mass parameter M. All the calculations are obtained with the parameters α, χ and κ as in Fig. 2 (c) and the values of the mass parameter M as indicated in the figure. The experimental values $S(J)$ for ^{192}Os are included for comparison.

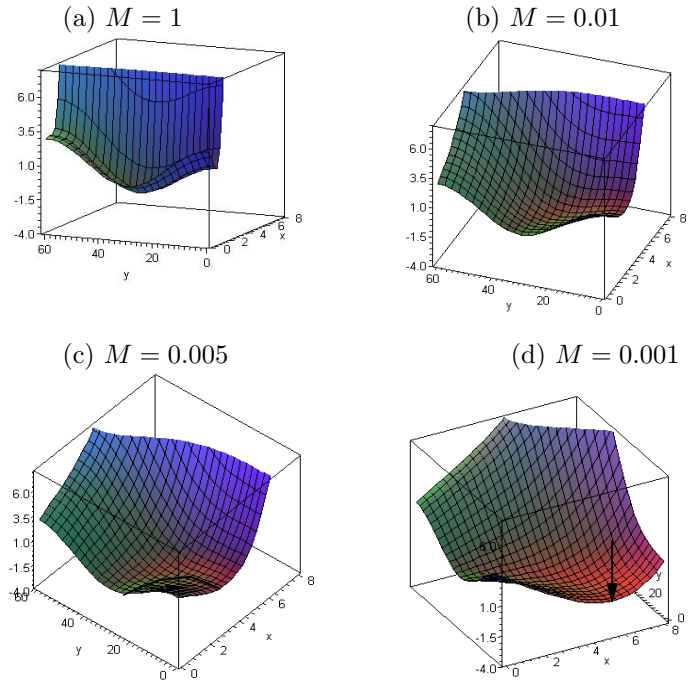

Fig. 11. Dependence of the potential energy surface on the mass parameter M. Calculations for (a) $M = 1$, (b) $M = 0.01$, (c) $M = 0.005$ and (d) $M = 0.001$ are shown. The remaining parameters are fixed to $\alpha = 1.5$, $\chi = 1$ and $\kappa = 3$. The values of the deformation parameter γ are shown on the y axis, while the x axis represents the deformation parameter β.

that drives the system towards an axially symmetric minimum. Indeed, we observe that with decreasing M the triaxial minimum flattens and eventually transforms into a whole region of competing γ values (as indicated by a thick line in Fig. 11 (c)) thus decreasing the effective γ deformation. For even smaller values of M, the absolute minimum of the potential will regain an axial symmetry (Fig. 11 (d), indicated by an arrow). Thus, it is clearly seen that increasing β fluctuations (decreasing M) acts against the triaxiality and leads to a gradual decrease of the magnitude of the triaxial staggering of the quasi-γ-band and changes it eventually into the one expected for an axially symmetric nucleus. On the other hand, in the axially symmetric regime β fluctuations act in an opposite way; increasing β fluctuations will produce an increasing magnitude of the staggering pattern.

4. Discussion

The ACM enables one to carry out easy collective model calculations for a diverse range of Hamiltonians and for essentially arbitrary values of β and γ stiffness. A primary objective of analyzing data within a model is to identify the model's deficiencies and suggest ways in which it could be improved. Obviously, this goal can only be achieved when many experimental spectra for various ACM Hamiltonians are analyzed. This work represents an attempt in this direction.

In an application to the Os isotopes, we have shown that a large amount of centrifugal stretching is observed when the β and γ vibrational bands appear in the low-energy domain. As pointed out by Rowe *et al.* [4], if this result were shown to persist for all reasonable ACM Hamiltonians that correspond to low-energy β or γ vibrational bands one would have to question the adiabatic approximation of the BM which completely neglects such coupling effects. In particular, it would be necessary to question the consistency of the interpretation of the low-lying excited bands as β or γ vibrational bands when the centrifugal stretching effects are observed to be small.

The absence of large centrifugal stretching effects in the experimental spectrum is even more significant than their absence in the adiabatic approximation to the model. This may indicate that real β bands of the model lie at a much higher energy. This conclusion is not only in agreement with a prediction of the vibration-rotation model which does not expect the β bandhead to be low in energy but also with the symplectic model calculations. In fact, in the absence of mixing of the valence SU(3) representations due to pairing, spin–orbit and other non-collective interactions the effective shell-model description of the low-lying collective states assigns different $K = 0$ bands to different SU(3) representations with no B(E2) transitions between them.

An analysis of experimental properties of the first excited 0^+ states indeed shows that only few of the 0_2^+ states may be interpreted as β vibrations [23]. Unlike the γ vibrations, the properties of the 0_2^+ states are more complex and depend sensitively on the changing Fermi surface. Also in the IBM, the 0_2^+ states are of a very different character than the β vibration [47]. In particular, in the SU(3) limit the $K = 0$ and 2 bands of the $(2N - 4, 2)$ representation are degenerate and transitions to the ground state band are forbidden. The QPM calculations that depend critically on the pairing part of the Hamiltonian have also confirmed that most of the 0_2^+ states cannot be regarded as β vibrations [48]. It is clear that more microscopic calculations that include the pairing and more experimental data of all kinds are needed before making any assignment.

From the perspective of the ACM and taking into account the available experimental information, we may conclude that in the case of ^{188}Os, a β vibration should be looked for at energies around or above 1700 keV. In the case of ^{192}Os, the situation is much more conclusive. The 0_4 excited state at 1924 keV stands out as the best candidate for a β vibration. To make a definitive conclusion, more experimental information about this state would be needed to verify the other properties expected to be satisfied by such a state.

An undesirable feature of the ACM calculations is an increasing shift of the whole γ band towards higher energies with increasing β stiffness of the potential. This question will be investigated in more detail in forthcoming ACM calculations.

We have also shown that a realistic description of quasi-γ-band staggering pattern requires a right amount of β fluctuations to be present in the model. In fact, models that are too β-rigid cannot reproduce correctly magnitudes of the quasi-γ-band staggering in the triaxial regime. Thus, while in the axially symmetric case staggering amplitudes decrease with increasing β rigidity of the model the opposite is true in the triaxial case. Similar conclusions can be expected for the role played by γ fluctuations of the potential in both regimes.

G.T. would like to thank D.J. Rowe and J L. Wood for many stimulating discussions. M.A. acknowledges financial support of the LPSC, Grenoble during her Master 2 internship. Technical help of M.M. Thiam is gratefully acknowledged.

REFERENCES

[1] A. Bohr, *Mat. Fys. Medd. K. Dan. Vidensk. Selsk.* **26**, No. 14 (1952).

[2] A. Bohr, B.R. Mottelson, *Nuclear Structure: Nuclear Deformations*, World Scientific, Singapore 1998, Vol. 2.

[3] F. Iachello, A. Arima, *The Interacting Boson Model*, Cambridge University Press, Cambridge 1987.

[4] D.J. Rowe, T.A. Welsh, M.A. Caprio, *Phys. Rev.* **C79**, 054304 (2009).

[5] D.J. Rowe, J.L. Wood, *Fundamentals of Nuclear Models; Foundational Models*, World Scientific, Singapore 2010, Vol. 2.

[6] M. Baranger, K. Kumar, *Nucl. Phys.* **A110**, 490 (1968).

[7] M. Baranger, K. Kumar, *Nucl. Phys.* **A110**, 529 (1968).

[8] M. Baranger, K. Kumar, *Nucl. Phys.* **A122**, 273 (1968).

[9] K.J. Weeks, T. Tamura, *Phys. Rev. Lett.* **44**, 533 (1980).

[10] M. Girod, B. Grammaticos, *Phys. Rev. Lett.* **40**, 361 (1978).

[11] I. Ragnarsson *et al.*, *Nucl. Phys.* **A233**, 329 (1974).

[12] G.A. Leander *et al.*, *Nucl. Phys.* **A400**, 97c (1983).

[13] K. Kumar, *Phys. Lett.* **B29**, 25 (1969).

[14] R.F. Casten, J.A. Cizewski, *Nucl. Phys.* **A309**, 477 (1978).

[15] A. Ansari, *Phys. Rev.* **C38**, 953 (1988).

[16] A. Ansari, *Phys. Rev.* **C33**, 321 (1986).

[17] L.M. Robledo, R. Rodriguez-Guzman, P. Sarriguren, *J. Phys. G: Nucl. Part. Phys.* **36**, 115104 (2009).

[18] A.A. Raduta, P. Buganu, *Phys. Rev.* **C83**, 034313 (2011).

[19] L. Fortunato, S. De Baerdemacker, K. Heyde, *Phys. Rev.* **C74**, 014310 (2006).

[20] J.M. Allmond *et al.*, *Phys. Rev.* **C78**, 014302 (2008).

[21] J. Carvalho, R. Le Blanc, M. Vassanji, D.J. Rowe, *Nucl. Phys.* **A452**, 240 (1986).

[22] R. Le Blanc, J. Carvalho, M. Vassanji, D.J. Rowe, *Nucl. Phys.* **A452**, 263 (1986).

[23] P.E. Garrett, *J. Phys. G: Nucl. Part. Phys.* **27**, R1 (2001).

[24] P.O. Hess, J.A. Maruhn, W. Greiner, *J. Phys. G: Nucl. Phys.* **7**, 737 (1981).

[25] G. Gneuss, W. Greiner, *Nucl. Phys.* **A171**, 449 (1971).

[26] M.A. Caprio, D.J. Rowe, T.A. Welsh, *Comput. Phys. Commun.* **180**, 1150 (2009).

[27] T.A. Welsh, unpublished (2008).

[28] D.J. Rowe, *Nucl. Phys.* **A735**, 372 (2004).

[29] D.J. Rowe, P.S. Turner, *Nucl. Phys.* **A753**, 94 (2005).

[30] M.A. Caprio, *Phys. Rev.* **C72**, 054323 (2005).

[31] D.J. Rowe, *Nuclear Collective Motion: Models and Theory*, Methuen, London 1970; reprinted by World Scientific, Singapore 2010.

[32] P.S. Turner, D.J. Rowe, *Nucl. Phys.* **A756**, 333 (2005).

[33] M.A. Caprio, *Phys. Rev.* **C83**, 064309 (2011).

[34] G. Rosensteel, D.J. Rowe, *Phys. Rev. Lett.* **38**, 10 (1977).

[35] Evaluated Nuclear Structure Data File (ENSDF database) `www.nndc.bnl.gov/ensdf/`

[36] P. Moeller, J.R. Nix, W.D. Myers, W.J. Swiatecki, *At. Data Nucl. Data Tables* **59**, 185 (1995).

[37] J.L. Wood, E.F. Zganjar, C. de Coester, K. Heyde, *Nucl. Phys.* **A651**, 323 (1999).

[38] W.R. Kane, R.F. Casten, D.D. Warner, *Phys. Lett.* **B117**, 15 (1982).

[39] J.M. Eisenberg, W. Greiner, *Nuclear Models*, Vol. 1, Norths-Holland, 1975.

[40] V.G. Soloviev, *Theory of Atomic Nuclei: Quasiparticles and Phonons*, Institute of Physics, Bristol, UK, 1992.

[41] N. Lo Iudice, A.V. Sushkov, *Phys. Rev.* **C78**, 054304 (2008).

[42] L. Wilets, M. Jean, *Phys. Rev.* **102**, 788 (1956).

[43] E.A. McCutchan, N.V. Zamfir, *Phys. Rev.* **C71**, 054306 (2005).

[44] E.A. McCutchan, D. Bonatsos, N.V. Zamfir, R.F. Casten, *Phys. Rev.* **C76**, 024306 (2007).

[45] N.V. Zamfir, R.F. Casten, *Phys. Lett.* **B260**, 265 (1991).

[46] G. Thiamova, *Eur. Phys. J.* **A45**, 81 (2010).

[47] R.F. Casten, D.D. Warner, *Rev. Mod. Phys.* **60**, 389 (1988).

[48] V.G. Soloviev, *Nucl. Phys.* **69**, 1 (1965).